# Exploiting the Kinematic Redundancy of a Backdrivable Parallel Manipulator for Sensing During Physical Human-Robot Interaction

Arda Yiğit, Tan-Sy Nguyen, Clément Gosselin

# Exploiting the Kinematic Redundancy of a Backdrivable Parallel Manipulator for Sensing During Physical Human-Robot Interaction

Arda Yiğit, Tan-Sy Nguyen and Clément Gosselin

***Abstract*— Robots need to adapt their behaviour while physically interacting with an operator to guarantee safety and provide intuitiveness. Inferring the intentions of the operator is a challenging problem that can be addressed by introducing sensors, in addition to motor encoders. Also, kinematic redundancy can be used to avoid issues such as singularities or mechanical interference, and the redundant coordinates can be controlled freely. In this work, we propose to use the redundant degrees of freedom to infer the intentions of an operator interacting with a backdrivable kinematically redundant parallel robot, without introducing any additional sensors. The proposed approach is based on the fact that, in mechanically backdrivable robots, the operator can control the redundant degrees of freedom, and this can be sensed using solely motor encoders through the solution of the forward kinematics. This approach is implemented to switch between a position controller and a controller that allows the operator to guide the robot freely thanks to gravity compensation. Experiments are carried out to compare this approach with an existing one and show that it improves intuitiveness during interaction by reducing false mode change detections.**

## I. Introduction

Physical human-robot interaction consists of a modality that can be used to adapt the behaviour of a robot in order to assist an operator while executing a given task. To this end, sensory data are needed to infer the intentions of the operator and to come up with a suited controller that yields the desired closed-loop dynamics.

Some industrial robots, such as Kuka LBR iiwa, Universal Robot UR5e or Fanuc CR to name a few, are equipped with both encoders and force sensors to perform active force control. They have operation modes during which they can be guided by an operator. In such modes, the controller only compensates for gravity, which requires an accurate model of the mass distribution. The operator needs to be in contact with the robot at all times, otherwise, because of modelling errors and external disturbances, the robot can move in an uncontrolled way. This causes safety issues and reduces the comfort and the intuitiveness of the interaction since the use of dead man's switch is then required. Adding more sensors can help to alleviate these issues.

While less common than encoders and force/torque sensors, other devices have also been used for physical human-robot interaction. Skin-like tactile sensors detect the human touch and the positions of the contacts [1], [2]. They can be mounted on the end-effector to ensure (or avoid) contact [3]. Robot links can be covered with low-impedance displacement sensors, similar to shells, to decouple the user interaction forces from gravitational and inertial loads [4]. The sensors can also be on the operator side, for example the operator can be equipped with inertial measurement units [5] or electromyographs [6].

Robots actuated by direct-drive motors can control the wrench generated at the end-effector without any force sensor. However, since there are no gearboxes, these motors are not adapted for serial architectures like industrial robot arms. In parallel robots, the actuators can be fixed to the base, reducing significantly the moving mass. However, parallel robots often suffer from singularities which restrict their workspace. Introducing kinematic redundancy can yield singularity-free mechanisms [7]. The additional degrees of mobility can then be used, for example, for the remote actuation of a gripper. Some parallel haptic devices have kinematically redundant designs to provide grasping capabilities [8], [9]. Two tripedal $(6+3)$-degree-of-freedom (DoF) parallel robots have been proposed recently by our research group for physical human-robot interaction [10], [11]. The robot developed by Wen et al. [10] is hybrid parallel, i.e., not all motors are fixed to the base. The mechanism is singularity-free within its reachable workspace thanks to its kinematically redundant architecture. Yiğit et al. [11] modified the leg architecture so that all motors are mounted on the base, reducing the moving mass while increasing the maximum wrench that can be generated at the end-effector by using more powerful actuators. In these robots, two of the three additional degrees of mobility are used to remotely operate a gripper at the end-effector. The remaining redundant degree of freedom can be freely controlled.

Robots performing physical human-robot interaction often need to switch between two operation modes. They can either be in "task mode", moving autonomously to track a reference trajectory, or be guided by an operator in "collaborative mode", for example, to teach positions for repetitive tasks. Detecting whether the operator intends to move the robot without introducing additional sensors is a challenging problem. Wen et al. proposed the use of a double threshold strategy [10]. The robot switches to collaborative mode during which the operator can guide the end-effector if either the tracking error or the velocity crosses some given thresholds. Otherwise, the robot is in task mode. While this strategy allows the detection of the presence of an operator when the robot is guided along trajectories at high speed, it suffers from many undesired and unexpected changes of

This work was supported by the Natural Sciences and Engineering Research Council of Canada (NSERC).

The authors are with the Department of Mechanical Engineering, Université Laval, Québec, QC, Canada. Emails: arda.yigit.1@ulaval.ca, tan-sy.nguyen.1@ulaval.ca, gosselin@gmc.ulaval.ca.

operation mode during slow trajectories for tasks requiring precision, significantly deteriorating the interaction.

Sensing the intention of the operator without using sensors other than motor encoders is a challenging problem. This work proposes a solution for kinematically redundant parallel backdrivable robots. Mechanically backdrivable robots can be operated by applying a force to the output (i.e., the end-effector) or to any other moving link of the robot. In particular, the operator can control the redundant degrees of freedom, which can be sensed with high precision using motor encoders. A similar approach was used in [12] for large payloads using an underactuated robotic system. In this work, the redundant degrees of freedom are used by the operator to switch between a position controller and an interaction controller. The experimental results are compared to those obtained with the double threshold strategy proposed by Wen et al. [10] and show the superiority of using the redundant link to detect the presence of an operator. It is noted that neither of these two approaches requires the use of a force/torque sensor because the robot is backdrivable.

This paper is structured as follows. First, a general dynamic model is derived in Section II for kinematically redundant parallel backdrivable robots both in open loop and in closed loop with an impedance controller, and the switching between operation modes is discussed. Then, the experimental setup is presented in Section III. Experimental results are shown in Section IV. Section V concludes the paper and discusses some perspectives.

## II. Modelling

Let us consider an $n$-DoF manipulator, which is kinematically redundant with respect to a given task that requires $m < n$ degrees of freedom. Let $\boldsymbol{q}(t) \in \mathbb{R}^n$ be the vector of actuated joint coordinates, $\boldsymbol{x}_t(t) \in \mathbb{R}^m$ the vector of task coordinates and $\boldsymbol{x}_r(t) \in \mathbb{R}^{n-m}$ a vector of redundant coordinates. The task coordinates and the redundant coordinates are assumed to be independent. Let $\boldsymbol{x}(t) = [\boldsymbol{x}_t(t)^T\ \boldsymbol{x}_r(t)^T]^T \in \mathbb{R}^n$ be the vector of augmented task coordinates.

Within the singularity-free workspace of the robot, the velocity model can be written as

$$\begin{bmatrix} \dot{\boldsymbol{x}}_t \\ \dot{\boldsymbol{x}}_r \end{bmatrix} = \underbrace{\begin{bmatrix} \boldsymbol{J}_t(\boldsymbol{q}) \\ \boldsymbol{J}_r(\boldsymbol{q}) \end{bmatrix}}_{\boldsymbol{J}(\boldsymbol{q})} \dot{\boldsymbol{q}} \tag{1}$$

where $\boldsymbol{J}_t(\boldsymbol{q}) \in \mathbb{R}^{m\times n}$ and $\boldsymbol{J}_r(\boldsymbol{q}) \in \mathbb{R}^{(n-m)\times n}$ are Jacobian matrices corresponding respectively to task coordinates and redundant coordinates. For all non-singular configurations, these matrices are well-defined and matrix $\boldsymbol{J}(\boldsymbol{q}) \in \mathbb{R}^{n\times n}$ is invertible.

### A. Open-loop Dynamics

In joint space, the dynamics of the robot can be written in the form

$$\boldsymbol{M}(\boldsymbol{q})\ddot{\boldsymbol{q}} + \boldsymbol{C}(\boldsymbol{q},\dot{\boldsymbol{q}})\dot{\boldsymbol{q}} + \boldsymbol{g}(\boldsymbol{q}) = \boldsymbol{\tau} - \boldsymbol{J}(\boldsymbol{q})^T \boldsymbol{f}_{ext} \tag{2}$$

where $\boldsymbol{M}(\boldsymbol{q}) \in \mathbb{R}^{n\times n}$ is the joint-space generalized inertia matrix, $\boldsymbol{C}(\boldsymbol{q},\dot{\boldsymbol{q}}) \in \mathbb{R}^{n\times n}$ the matrix of Coriolis and centrifugal effects, $\boldsymbol{g}(\boldsymbol{q}) \in \mathbb{R}^n$ the vector of conservative forces, $\boldsymbol{\tau} \in \mathbb{R}^n$ the vector of motor forces (or torques) and $\boldsymbol{f}_{ext} \in \mathbb{R}^n$ the vector of external wrench applied on the robot.

In augmented task space, (2) becomes

$$\boldsymbol{\Lambda}(\boldsymbol{q})\ddot{\boldsymbol{x}} + \boldsymbol{\Gamma}(\boldsymbol{q},\dot{\boldsymbol{q}})\dot{\boldsymbol{x}} + \boldsymbol{\eta}(\boldsymbol{q}) = \boldsymbol{J}(\boldsymbol{q})^{-T}\boldsymbol{\tau} - \boldsymbol{f}_{ext} \tag{3}$$

with $\boldsymbol{\Lambda} = \boldsymbol{J}^{-T}\boldsymbol{M}\boldsymbol{J}^{-1}$, $\boldsymbol{\Gamma} = \boldsymbol{J}^{-T}\boldsymbol{C}\boldsymbol{J}^{-1} - \boldsymbol{\Lambda}\dot{\boldsymbol{J}}\boldsymbol{J}^{-T}$ and $\boldsymbol{\eta} = \boldsymbol{J}^{-T}\boldsymbol{g}$ [13].

### B. Closed-loop Dynamics

The actuated joint coordinates $\boldsymbol{q}$ are measured using motor encoders. The joint velocities $\dot{\boldsymbol{q}}$ can either be measured or estimated using a state observer — for example an extended Kalman filter. In the latter case, the observability needs to be verified, assuming, for example, that the external wrench $\boldsymbol{f}_{ext}$ is constant.

The following impedance control law is implemented to track the reference trajectory $\boldsymbol{x}^*$:

$$\begin{aligned}\boldsymbol{\tau} = \boldsymbol{J}(\boldsymbol{q})^T [&\boldsymbol{\Lambda}(\boldsymbol{q})\ddot{\boldsymbol{x}}^* + (\boldsymbol{\Gamma}(\boldsymbol{q},\dot{\boldsymbol{q}}) + \boldsymbol{D})(\dot{\boldsymbol{x}}^* - \dot{\boldsymbol{x}}) \\ &+ \boldsymbol{K}(\boldsymbol{x}^* - \boldsymbol{x}) + \boldsymbol{\Gamma}(\boldsymbol{q},\dot{\boldsymbol{q}})\dot{\boldsymbol{x}} + \boldsymbol{\eta}(\boldsymbol{q})]\end{aligned} \tag{4}$$

where matrices $\boldsymbol{D} \in \mathbb{R}^{n\times n}$ and $\boldsymbol{K} \in \mathbb{R}^{n\times n}$ are positive semidefinite.

Let $\boldsymbol{\xi} = \boldsymbol{x}^* - \boldsymbol{x}$ be the tracking error. Closed-loop dynamics are obtained by combining (3) and (4), yielding

$$\boldsymbol{\Lambda}(\boldsymbol{q})\ddot{\boldsymbol{\xi}} + (\boldsymbol{\Gamma}(\boldsymbol{q},\dot{\boldsymbol{q}}) + \boldsymbol{D})\dot{\boldsymbol{\xi}} + \boldsymbol{K}\boldsymbol{\xi} = \boldsymbol{f}_{ext}. \tag{5}$$

The passivity with respect to the pair $(\boldsymbol{f}_{ext}, \dot{\boldsymbol{\xi}})$ can be guaranteed using the positive semidefinite storage function

$$V = \frac{1}{2}\dot{\boldsymbol{\xi}}^T\boldsymbol{\Lambda}(\boldsymbol{q})\dot{\boldsymbol{\xi}} + \frac{1}{2}\boldsymbol{\xi}^T\boldsymbol{K}\boldsymbol{\xi}. \tag{6}$$

Since matrix $\frac{1}{2}\dot{\boldsymbol{\Lambda}} - \boldsymbol{\Gamma}$ is skew-symmetric [13], it yields

$$\dot{V} \leq \dot{\boldsymbol{\xi}}^T\boldsymbol{f}_{ext} \tag{7}$$

for any constant positive semidefinite matrix $\boldsymbol{K}$ and possibly time-varying positive semidefinite matrix $\boldsymbol{D}$. Therefore, the closed-loop system (5) is passive with respect to the pair $(\boldsymbol{f}_{ext}, \dot{\boldsymbol{\xi}})$, and it can be coupled to any passive environment without hindering passivity [14].

### C. Operation Modes

The robot has two operation modes: collaborative mode and task mode. The operation mode to be used is determined based on the redundant coordinates $\boldsymbol{x}_r$. The robot controller is represented schematically in Fig. 1. Matrices $\boldsymbol{K}_{collab}$ and $\boldsymbol{K}_{task}$ determine the virtual stiffness in respectively collaborative and task modes. The switching function is described in Section III-B.

Let us choose $\boldsymbol{K}$ with the form

$$\boldsymbol{K} = \begin{bmatrix} \boldsymbol{K}_t & \boldsymbol{0} \\ \boldsymbol{0} & \boldsymbol{K}_r \end{bmatrix} \tag{8}$$

with $\boldsymbol{K}_t \in \mathbb{R}^{m\times m}$ and $\boldsymbol{K}_r \in \mathbb{R}^{(n-m)\times(n-m)}$ positive semidefinite matrices.

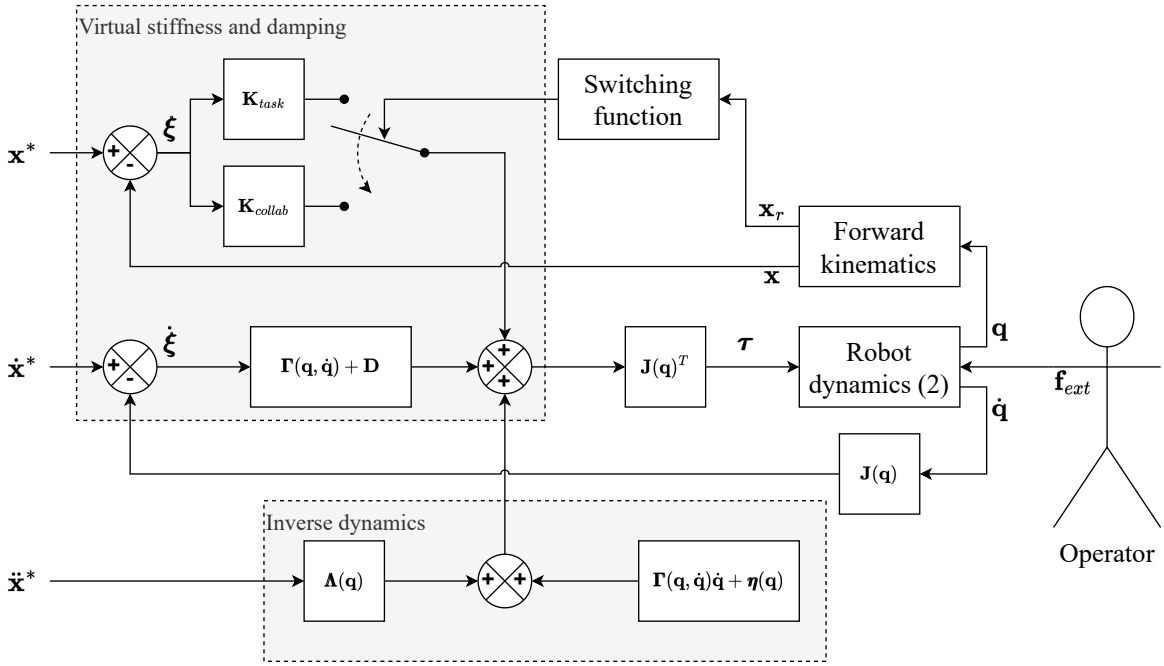


Fig. 1. Control diagram of the robot.

In collaborative mode, matrix $\boldsymbol{K}_t$ is set to zero and the reference trajectory $\boldsymbol{x}_t^*$ is constant, i.e., $\dot{\boldsymbol{x}}_t^* = \mathbf{0}$ and $\ddot{\boldsymbol{x}}_t^* = \mathbf{0}$. As a consequence, the robot follows the movements of the operator. This mode can be used, for example, to teach some poses to the robot.

In task mode, matrix $\boldsymbol{K}_t$ is positive definite. Hence, the robot follows the reference trajectory $\boldsymbol{x}_t^*$. This mode can be used, for example, to keep the robot still when the operator is not interacting with it or to replay/repeat the taught positions.

Note that the proposed proof for passivity is not valid when switching the operation mode since the stiffness matrix $\boldsymbol{K}_t$ associated with the task variables is no longer constant. To prevent losing passivity, in this work, it is assumed that the switching between the operation modes only happens when the task coordinates are (i) at steady state (so $\dot{\boldsymbol{\xi}}_t = \mathbf{0}$) and (ii) without steady-state error, i.e., $\boldsymbol{\xi}_t = \mathbf{0}$, where $\boldsymbol{\xi}_t = \boldsymbol{x}_t^* - \boldsymbol{x}_t$ is the tracking error in task coordinates. Since $\boldsymbol{\xi}_t = \mathbf{0}$, matrix $\boldsymbol{K}_t$ has no impact on (5). Therefore, varying $\boldsymbol{K}_t$ does not violate passivity. A less conservative approach could consist in changing the stiffness smoothly and considering other storage functions [15], [16] or tank-based methods [17], [18]. However, this is out of the scope of this paper.

## III. Experimental Setup

The control and interaction technique presented above is validated experimentally. This section describes the robot that is used for the experiments and the implementation of the operation mode switching procedure.

### A. Backdrivable Kinematically Redundant Parallel Robot

Experiments are carried out using a tripedal $(6+3)$-DoF kinematically redundant hybrid parallel robot developed in [10] for intuitive physical human-robot interaction (see Fig. 2). Using only three legs reduces mechanical interference. Each leg is equipped with three direct-drive motors, one of them is fixed, and the other two are mobile and drive a planar five-bar linkage that constitutes a leg of the robot. Mobile motors are positioned close to the base to reduce the moving inertia. The leg mechanism is singularity-free within its reachable workspace. The legs are attached through spherical joints $S_i$ ($i \in \{1,2,3\}$) to a configurable platform with three degrees of mobility.

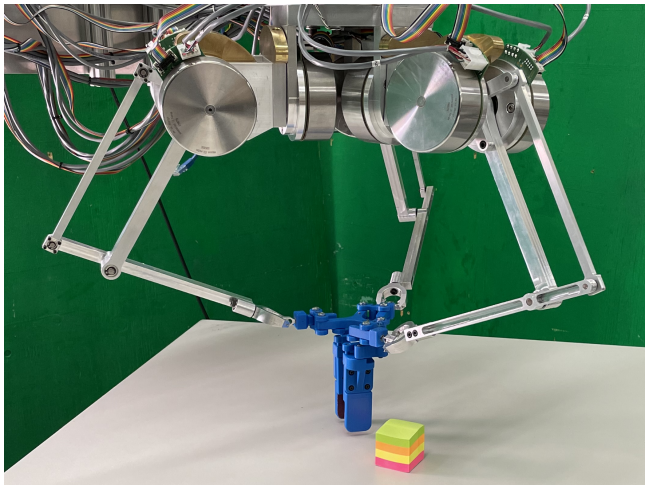

Fig. 2. Backdrivable tripedal $(6+3)$-DoF kinematically redundant hybrid parallel robot proposed in [10].

Figure 3 is a simplified diagram of the platform. The platform consists of an equilateral triangle of side length $l_1$ with revolute joints $R_i$ at the vertices. The spherical joints $S_i$ are connected to the revolute joints $R_i$ through identical

links of length $l_2$. Using Grassmann line geometry, it can be readily observed that the configurable platform is singular only if (i) spherical joints $S_i$ are aligned or (ii) all three lines $(R_i, S_i)$ have a common intersection [10]. The former condition cannot happen since the dimensions are selected such that $l_2 < \frac{\sqrt{3}}{4} l_1$. The latter condition is prevented using mechanical stops such that $\psi_{min} \leq \psi_i \leq \psi_{max}$, with $\psi_{min} > 0°$ and $\psi_{max} < 120°$. As a consequence, the robot has no singularities within its reachable workspace.

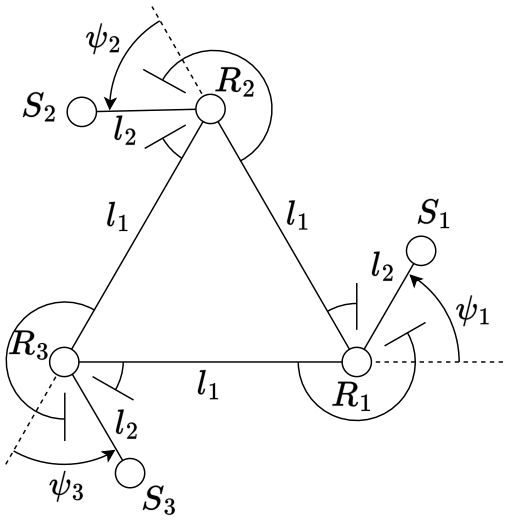


Fig. 3. Configurable 3-DoF platform [10]. The physical joint limits of the redundant coordinates $\psi_i$ are indicated.

Equipped with direct-drive motors, this mechanism has a very low mechanical impedance and is backdrivable, which means that an operator can easily move the platform without an active help of the motors.

The robot has eight task coordinates, six corresponding to the pose $\boldsymbol{p}$ of the end-effector and two ($\psi_1$ and $\psi_2$) that control the opening of a gripper: $\boldsymbol{x}_t = \begin{bmatrix} \boldsymbol{p}^T & \psi_1 & \psi_2 \end{bmatrix}^T$. The only redundant coordinate is the angle of the link that is not related to the gripper: $x_r = \psi_3$.

The experiments are designed such that, in task control mode, there are no physical interactions with either the operator or the environment (except with the objects to be grasped). As a consequence, the positive definite stiffness matrix $\boldsymbol{K}_t$ associated with the task variables $\boldsymbol{x}_t$ does not need to be tuned finely. For the experiments, this matrix is diagonal:

$$\boldsymbol{K}_t = \mathrm{diag}(100, 100, 100, 50, 50, 50, 10, 10). \qquad (9)$$

The damping matrix is also diagonal:

$$\boldsymbol{D} = \mathrm{diag}(5, 5, 5, 0.1, 0.1, 0.1, 0.1, 0.1, 0). \qquad (10)$$

The coefficients of matrices $\boldsymbol{K}_t$ and $\boldsymbol{D}$ are expressed in standard SI units.

The closed-loop behaviour of the redundant DoF $x_r$ is similar to that of trigger buttons on game controllers. While the operator is not moving the redundant link, the virtual stiffness $k_r$ maintains the redundant link at a mechanical stop, i.e., $x_r = \psi_{min}$ (respectively $x_r = \psi_{max}$). To generate a minimum torque below which the redundant link stays in contact with the mechanical stop, the reference position can be chosen beyond the mechanical limit: $x_r^* < \psi_{min}$ (respectively $x_r^* > \psi_{max}$). The values of both $k_r$ and $x_r^*$ can be selected to provide comfort to the operator and to avoid undesired movements of the redundant link during task control mode due to inertial effects, which might cause unexpected mode switching. For the experiments, the stiffness is $k_r = 2\,\mathrm{N\,rad^{-1}}$ and the reference is $x_r^* = 30°$.

Note that, during the experiments, the stiffness associated with the redundant variable is generated virtually by active force control, but it is also possible to achieve this passively using a real spring.

### *B. Operation Mode Switching*

In order to switch from task mode to collaborative mode, the operator needs to move the redundant link from the equilibrium position to the opposite mechanical stop. The orientation of the redundant link $\psi_3$ is obtained from motor encoders by solving the forward kinematics in real time. If the value of the redundant coordinate crosses a given threshold value, the controller switches to the collaborative mode. To avoid multiple undesired mode changes in a short time window, a Schmitt trigger — also known as comparator with hysteresis — is used. The threshold values are at $40°$ and $50°$. During the collaborative mode, if the operator releases the redundant link, the controller switches back to task mode due to the virtual stiffness associated with the redundant task coordinate $x_r$. The transition between task mode and collaborative mode is schematically illustrated in Fig. 4.

The proposed approach to switch the operation mode is compared to an existing method proposed in [10], which implemented a double threshold strategy. For each actuated joint coordinate $q_i$, the first threshold is on the tracking error $q_i^* - q_i$ and the second threshold is on the joint velocity $\dot{q}_i$. During the experiments, the reference trajectory is static. Therefore, if the robot moves such that a threshold is crossed by any of the actuated joints, the robot switches to collaborative mode, and, otherwise, it is in task mode. Both threshold values are tuned to provide the best possible user experience. The second threshold (on the joint velocity) defines a minimum velocity below which the robot can switch between modes unexpectedly. This phenomenon is a significant drawback for tasks requiring precision, and it can be observed on the video accompanying the paper [10]. In the next section, this unexpected behaviour is highlighted in experimental data.

## IV. Experiments

Two approaches to switch the controller mode, namely the newly proposed approach using the redundancy and the existing one based on the double threshold, are compared using a "teach and repeat" experiment for pick-and-place tasks. The video accompanying this paper shows the experiments. To simplify the experiments, two assumptions

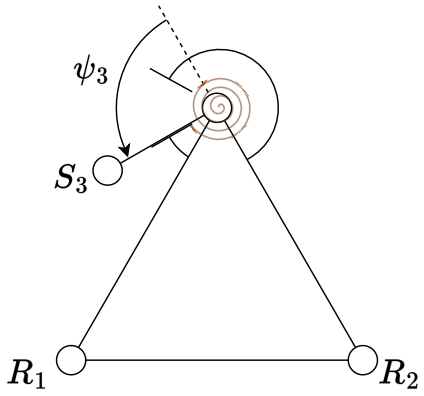


(a) The virtual torsion spring maintains the redundant link at a mechanical stop when there is no interaction. The controller is in task mode.

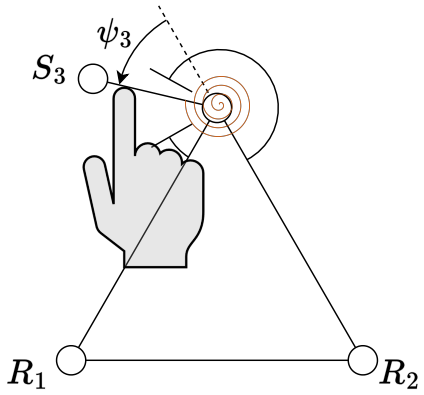


(b) The operator moves the redundant link towards the opposite mechanical stop. The controller switches to collaborative mode.

Fig. 4. The operator changing the controller mode. The torsion spring pulls the redundant link to the mechanical stop at $\psi_{max}$. The controller switches to the collaborative mode when the operator pushes the redundant link towards the mechanical stop at $\psi_{min}$.

are made: (i) the matrix of Coriolis and centrifugal effects $\boldsymbol{\Gamma}(\boldsymbol{q}, \dot{\boldsymbol{q}})$ in augmented task space is neglected since the movements are slow and the moving inertia is small and (ii) the opening of the gripper is assumed to be known for each waypoint. During the teaching phase of the experiment, when the robot is in task mode, the task reference $\boldsymbol{x}_t^*$ remains constant. It maintains the value that was measured when the controller switched from collaborative mode to task mode and, therefore, the robot remains stationary until the next interaction is initiated.

The procedure to teach a waypoint consists of the following steps:

1) The operator makes the robot switch from task mode to collaborative mode. In the proposed approach, this transition is detected by the redundant coordinate $\psi_3$ crossing the higher threshold of the Schmitt trigger (i.e., when $\psi_3 > 40°$). In the double threshold approach, the transition is detected either by the minimum velocity of the actuated joints becoming higher than $0.2\,\mathrm{rad/s}$ or the minimum tracking error being higher than $0.1\,\mathrm{rad}$.

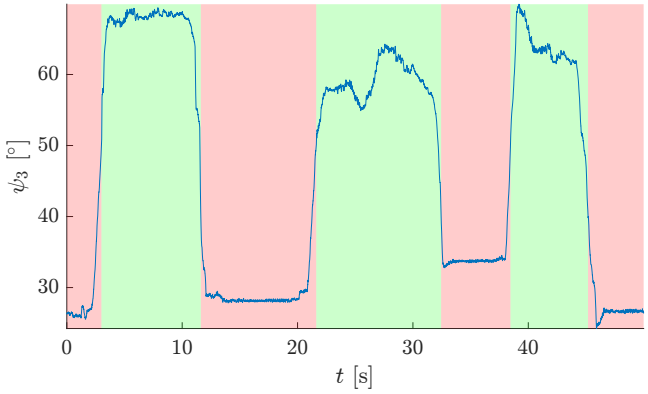


Fig. 5. Waypoint teaching experiment using the redundancy-based approach to switch between controller modes.

2) The operator moves the robot to the next waypoint.

3) The operator makes the robot switch from collaborative mode to task mode. In the proposed approach, this transition is detected by the redundant coordinate $\psi_3$ crossing the lower threshold of the Schmitt trigger (i.e., when $\psi_3 < 30°$). In the double threshold approach, this transition is detected when the maximum velocity of the actuated joints becomes lower than $0.2\,\mathrm{rad/s}$.

4) The controller records the waypoint.

For each waypoint, the operation mode needs to change only twice. Therefore, for $n$ waypoints, $2n$ transitions are expected. The video accompanying this paper illustrates pick-and-place tasks with a single object using each of the two approaches to change the operation mode. During the experiments, three waypoints are used: a pose where the object is to be grasped, a pose where the object is to be dropped and an intermediate pose.

The results of the teaching experiment using the redundancy-based approach are shown in Fig. 5. The red and green areas represent respectively the task mode and the collaborative mode. Transitions are obtained from the redundant joint coordinate $\psi_3$, as illustrated in Fig. 4. It can be noticed that the operation mode changes six times, therefore, there are no undesired transitions.

As explained in Section III, the use of a threshold on joint velocities for the double threshold-based approach suggests that this method would lead to numerous undesired operation mode changes. This is confirmed experimentally as it can be seen in Fig. 6, where the double threshold-based switching function (DT-B SF) replaces the redundancy-based one. The operation mode changes 84 times. Here, the red areas correspond to the periods of time during which the operator is away from the end-effector and the green areas to the period of time during which the operator is in contact with the end-effector. The transition times are approximated using the video recording. As it can be seen in the video, switching back to collaborative mode after an undesired change may not be immediate. Therefore, the operator may still be in contact with the robot even if the controller switched back to task mode. As an example, between times $t_0 = 19.3\,\mathrm{s}$ and $t_1 = 21.8\,\mathrm{s}$, the controller stayed in task mode while the

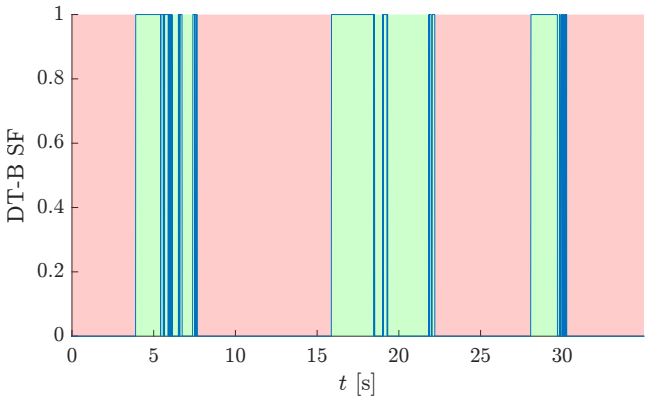


Fig. 6. Waypoint teaching experiment using the double threshold-based switching function (DT-B SF). Areas are respectively red or green when the operator is away from or in contact with the end-effector.

operator was attempting to move the end-effector.

## V. Conclusion and Perspectives

This work introduces a novel approach to detect the intentions of an operator interacting with kinematically redundant backdrivable parallel robots using only motor encoders. Such robots can be guided by operators without requiring force/torque sensors. In particular, the operator can control the redundant degrees of freedom, which can be sensed using the forward kinematics. The controller can, then, adapt its behaviour accordingly.

This approach has been tested experimentally on a $(6+3)$-DoF hybrid parallel robot with an impedance controller that switches between two operation modes: a collaborative mode during which the operator can guide the robot and a task mode during which the robot is stiff. Sufficient conditions are given under which passivity is conserved while switching between the two modes. Comparisons with an existing method using thresholds on joint tracking error and velocities show the effectiveness of the proposed approach, reducing significantly the number of false operation mode changes.

Although the proposed method has shown its effectiveness, there is still room for improvement and several potential research directions can be identified.

The proof for passivity yields a very conservative condition that could be less restrictive using state-of-the-art storage functions [15]–[17]. This would allow for varying the virtual impedance parameters of the robot continuously. Indeed, in this work, only a binary signal was extracted from the coordinate associated with the redundant degree of freedom, since the robot needs to be static while changing the virtual stiffness with the given passivity condition.

The end-effector that is used for the robot was not specifically designed so that the operator can easily control the redundant link. Moreover, if the gripper mechanism uses only one degree of mobility, this leaves two redundant degrees of freedom that can be used for the interaction. Specific platforms could be designed to benefit from the redundant degrees of freedom. The interaction with the redundant degrees of freedom is not limited to presence detection or variable impedance, it can also be used, for example, as a low-impedance displacement sensor [4], [12]. These research directions have the potential to significantly improve the effectiveness of the proposed method, and they will be investigated in future work.

## References

[1] V. Duchaine, N. Lauzier, M. Baril, M.-A. Lacasse, and C. Gosselin, "A flexible robot skin for safe physical human robot interaction," in *Proceedings of the IEEE International Conference on Robotics and Automation*. IEEE, 2009, pp. 3676–3681.

[2] B. D. Argall and A. G. Billard, "A survey of Tactile Human–Robot Interactions," *Robotics and Autonomous Systems*, vol. 58, no. 10, pp. 1159–1176, 2010.

[3] A. Campeau-Lecours, "Développement d'algorithmes de commande et d'interfaces mécatroniques pour l'interaction physique humain-robot," Ph.D. dissertation, Université Laval, Québec, 2012.

[4] T. Laliberté and C. Gosselin, "Low-Impedance Displacement Sensors for Intuitive Physical Human–Robot Interaction: Motion Guidance, Design, and Prototyping," *IEEE Transactions on Robotics*, vol. 38, no. 3, pp. 1518–1530, 2022.

[5] J. A. Corrales, F. A. Candelas, and F. Torres, "Hybrid tracking of human operators using IMU/UWB data fusion by a Kalman filter," in *Proceedings of the ACM/IEEE international conference on Human robot interaction*, 2008, pp. 193–200.

[6] M. Bednarczyk, H. Omran, and B. Bayle, "EMG-Based Variable Impedance Control With Passivity Guarantees for Collaborative Robotics," *IEEE Robotics and Automation Letters*, vol. 7, no. 2, pp. 4307–4312, 2022.

[7] C. Gosselin, T. Laliberté, and A. Veillette, "Singularity-Free Kinematically Redundant Planar Parallel Mechanisms With Unlimited Rotational Capability," *IEEE Transactions on Robotics*, vol. 31, no. 2, pp. 457–467, 2015.

[8] P. Lambert and J. L. Herder, "A 7-DOF redundantly actuated parallel haptic device combining 6-DOF manipulation and 1-DOF grasping," *Mechanism and Machine Theory*, vol. 134, pp. 349–364, 2019.

[9] P. Lambert, L. Da Cruz, and C. Bergeles, "Design, Modeling, and Implementation of a 7-DOF Cable-Driven Haptic Device With a Configurable Cable Platform," *IEEE Robotics and Automation Letters*, vol. 5, no. 4, pp. 5764–5771, 2020.

[10] K. Wen, T. S. Nguyen, D. Harton, T. Laliberté, and C. Gosselin, "A Backdrivable Kinematically Redundant (6+3)-Degree-of-Freedom Hybrid Parallel Robot for Intuitive Sensorless Physical Human-Robot Interaction," *IEEE Transactions on Robotics*, vol. 37, no. 4, pp. 1222–1238, 2021.

[11] A. Yigit, D. Breton, Z. Zhou, T. Laliberté, and C. Gosselin, "Kinematic Analysis and Design of a Novel (6+3)-DoF Parallel Robot with Fixed Actuators," in *Proceedings of the IEEE International Conference on Robotic and Automation*, 2023.

[12] P. D. Labrecque, T. Laliberté, S. Foucault, M. E. Abdallah, and C. Gosselin, "uMan: A Low-Impedance Manipulator for Human–Robot Cooperation Based on Underactuated Redundancy," *IEEE/ASME Transactions on Mechatronics*, vol. 22, no. 3, pp. 1401–1411, 2017.

[13] L. Villani and J. De Schutter, "Force Control," in *Springer Handbook of Robotics*. Berlin, Heidelberg: Springer Berlin Heidelberg, 2008, pp. 161–185.

[14] J. E. Colgate and N. Hogan, "Robust control of dynamically interacting systems," *International Journal of Control*, vol. 48, no. 1, pp. 65–88, 1988.

[15] K. Kronander and A. Billard, "Stability Considerations for Variable Impedance Control," *IEEE Transactions on Robotics*, vol. 32, no. 5, pp. 1298–1305, 2016.

[16] M. Bednarczyk, H. Omran, and B. Bayle, "Passivity Filter for Variable Impedance Control," in *Proceedings of the IEEE/RSJ International Conference on Intelligent Robots and Systems*, 2020, pp. 7159–7164.

[17] F. Ferraguti, C. Secchi, and C. Fantuzzi, "A tank-based approach to impedance control with variable stiffness," in *Proceedings of the IEEE International Conference on Robotics and Automation*, 2013, pp. 4948–4953.

[18] C. Saudrais, L. Barbé, and B. Bayle, "Rate Mode Bilateral Teleoperation Based on Passivity Tanks and Variable Admittance Control," in *Proceedings of the IEEE International Conference on Robotics and Automation*, 2021, pp. 3942–3948.